Global stability of single-layer reticulated domes based on the valency of structural elements

Ranjith Kolakkattil[1], Konstantinos Daniel Tsavdaridis [2], Arul Jayachandran Sanjeevi [3]

Abstract

In general, parameters such as member slenderness, rise-to-span ratio, and support conditions determine the global stability of single-layer reticulated domes. The effect of member connectivity on the global and local stability of reticulated domes is usually not considered, even though they play a vital role. Hence, this paper examines the global stability of single-layer reticulated dome configurations based on the valences of vertices, edges, and faces. These valences are derived from the interrelation between the elements within a configuration. Valency is the number of specified elements connected to a different element. The valency plays a vital role in determining a reticulated dome's global stability as the interconnections ensure the smooth flow of load from the applied location to the support. Hence, the global stability of different single-layer configurations with different valences of vertices, edges, and faces is examined with different loading and support conditions. Different valences for selected dome configurations are calculated during the initial stage. Then the global stability of the dome configurations under different loading and support conditions is analyzed. The relation between the valency and the stability of dome configurations is analyzed to identify the stable dome configurations under various load conditions. Valency information helps to recognize the type of failure in the domes and reduces the probability of failure by altering the data to obtain an efficient configuration.

1. Introduction

Reticulated domes are spatial structures used to cover large volumes with the least surface area. The double curvature makes them one of the most efficient structures to cover large column-free spaces. The demand for the domes comes from both efficiency and aesthetics. Advancements in fabrication methods and efficient connection systems have considerably reduced construction time. They are used to cover large column-free areas like museums, art galleries, petroleum storage tanks, observatories, and stockpiles (Fig. 1). The spherical surface is used as the surface of revolution in most cases. The resistance provided by the structure against the load is through

---

[1] PhD Candidate, Department of Civil Engineering, Indian Institute of Technology Madras, Chennai, India
<ranjithk@alumni.iitm.ac.in>
[2] Professor, Department of Civil Engineering, School of Mathematics, Computer Science and Engineering, City University of London, United Kingdom <konstantinos.tsavdaridis@city.ac.uk>
[3] Professor, Department of Civil Engineering, Indian Institute of Technology Madras, Chennai, India
<aruls@civil.iitm.ac.in>

membrane action, and most of the members are primarily subjected to the axial force. The axial force ensures maximum utilization of the members' capacity and the resulting structure's high strength to weight ratio.

Figure 1: Interior view of the ring stockpile dome in Merida (Geometrica Inc., 2008)

Many single-layer dome configurations are constructed with triangles as a basic unit, as triangulation provides the most stable structure (Makowski 1986). The difference between triangulated structures and non-triangulated configurations is the variation in their member connectivity. Dome configuration changes when there is a modification in connectivity between the members. The studies related to the stability of single-layer reticulated shells are based on member slenderness, rise-to-span ratio, and connection rigidity. The importance of member connectivity is seldom studied.

The general instability behaviors in single-layer reticulated shells are broadly classified as geometrical factors and behavioral factors (Gioncu and Balut 1992). The shell geometry and the mesh density are the geometrical factors. The behavioral factors are instability forms, geometrical and material nonlinearities, imperfections, joint stiffness, and load distributions. A majority of the studies on single-layer reticulated shells are on behavioral factors, where the global and the local instabilities are comprehensively examined.

The stability of reticulated shells is studied based on continuum shell analogy theory, finite element methods, and experimental methods. Direct formulas are available to find the load-carrying capacity of the lattice structure when it is converted into an equivalent continuum shell (IASS working group 8 report 1985; Saitoh et al. 1986; and Suzuki et al. 1992). However, the conversion of discrete structures to continuum shells was not accurate, and it was challenging to find equivalent shell structures for the lattice structures.

The reticulated domes' global stability behavior depends on the buckling of a single member (Tanaka et al. 1985). The experimental studies showed that the slenderness of the members could cause the failure (Lenza 1992). Kani and Heidari (2007) described the automatic calculation of the bifurcation path of reticulated domes. A study on the progressive collapse of the domes due to the dynamic propagation of snap-through buckling found that the impact of dynamic snap-through is higher for pin-jointed domes than rigid-jointed domes (Abedi and Parke 1996). The single-layer dome configurations with non-triangulated patterns were more sensitive to dynamic snap-through than the domes with triangulated patterns. Yamada et al. (2001) examined imperfection sensitivities in single-layer lattice domes. Lopez et al. (2007) conducted a numerical and experimental investigation on a single-layer reticulated dome with semi-rigid joints. The study considered the effect of factors like dome geometry, member slenderness, joint rigidity, and load distribution. The study established the influence of geometric parameters on the global stability of dome structures.

The joint rigidity influences the load capacity of the single-layer shell domes to a great extent (Kato et al. 1998, Lopez et al. 2007, and Ma et al. 2015). Members in a dome are interconnected by a pin, semi-rigid, or rigid connection. Usually, semi-rigid or rigid connections are adopted for single-layer shells (IASS WG 8, 2014). Domes with semi-rigid joints will have lesser load capacity compared to domes with rigid joints. The joint stiffness also plays a crucial role in shaping the grid structures (Tsavdaridis et al. 2020).

Finite element software packages assist in conducting Geometrically Nonlinear Analysis (GNA), Geometrically and Materially Nonlinear Analysis (GMNA), and Geometrically and Materially Nonlinear Imperfection Analysis (GMNIA). Finite element analysis becomes more accessible and faster with technological advancements in computational tools. These packages help to understand the elastic and elastoplastic behavior of reticulated domes efficiently. Numerous studies on single-layer dome configurations based on finite element analysis have been conducted in recent times. The elastoplastic stability analysis of single-layer reticulated domes found that the buckling mode can change with the rise-to-span ratios (Fan et al. 2010). The elastoplastic stability also depends on the initial curvature of the members (Fan et al. 2012). The examination of the interaction between member buckling and overall buckling resulted in two types of instability patterns. They are progressive instability and synchronous instability (Yan et al. 2016). The member buckling occurs before the overall buckling in progressive instability, and the member buckling and the overall buckling co-occurs in synchronous instability.

The past studies have predominantly focused on the impact of member slenderness, joint rigidity, initial imperfection, geometrical and material nonlinearity, and load distributions. The study on the effect of member arrangement on stability is limited. There are tools and algorithms available to create a wide variety of single-layer dome configurations. The Formex Algebra is an excellent example of configuration processing (Nooshin and Disney 2000). Various shell configurations can be generated from the software developed based on Formex Algebra. Even though there are tools to create a wide variety of shell configurations, the fundamental reason why there is a difference in the load capacity for various configurations is seldom studied. Hence, a dome's basic elements and parameters become significant for explaining its behavior. A structure or a configuration can be defined by the basic elements of vertices, edges, faces, and cells. Parameters of structures are based on the interrelation between these elements (Loeb 2012).

These parameters are used to create different types of configurations (Kolakkattil et al. 2021). The variation in parameters is relevant while comparing the overall resistance of reticulated cylindrical shells by changing the connectivity between the members (Kolakkattil et al. 2021).

The dependence of parameter "valency" on the overall resistance of single-layer dome configurations helps to identify the optimum connectivity within structures with double curvature. Hence, this paper examines the effect of average edge valency of vertices and average edge valency of faces on the overall resistance of the structure.

2. Parameters used to define a configuration

The basic parameters of a configuration will help to explain the variation in load capacity of different single-layer domes. A configuration is a combination of elements - vertices, edges, faces, and cells. These elements help to identify the parameters within a structure. These parameters are dimensionality, valency, and extent (Loeb 2012).

The first parameter, dimensionality, is the degree of freedom of elements within a structure. For example, the dimensionality of a vertex and an edge are zero and one, respectively. Similarly, the dimensionality of a face and a cell are two and three, respectively. The second parameter, valency, is defined as the number of elements of a given dimensionality that meet an element of another dimensionality. The edge valency of each vertex in a hexagon is two, as each vertex is directly connected to two edges (Fig. 2). Similarly, the vertex valency of the face is six as there are six vertices for the hexagon. Different elements create different valences with the remaining elements in a structure (Table 1). The third parameter, extent, indicates measurable quantities like length, area, and volume. The total length and the total weight of the structures are defined based on this parameter. This parameter is significant due to its direct relation to total construction cost.
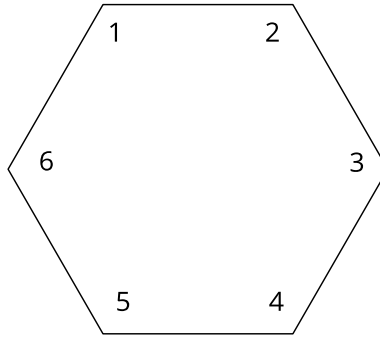
Figure 2: Vertex valency explained with a hexagon

Table 1: Different valences in a structure

Element	Vertex Valency	Edge Valency	Face Valency	Cell Valency
Vertex	-	V_1	V_2	V_3
Edge	2	-	E_2	E_3
Face	F_0	F_1	-	2
Cell	C_0	C_1	C_2	-

The variation in any of these parameters will modify the configuration. The overall resistance of the structure will change as a result of this modification. Hence, the study of these parameters helps to predict their impact on the resistance of a dome. The effect of the parameter "valency" is studied in this paper. The variation of the valency helps to create different configurations, which in turn helps to choose the required configuration based on the resistance required for a structure. A unique nomenclature is provided for single-layer dome configurations based on the valency of the vertices (Kolakkattil et al. 2021). If the edge valency of all the faces in a configuration is identical, the edge valency of vertices is arranged clockwise to derive the nomenclature. Hence, the nomenclature assigned for the three-sided face is V.4.3.3 (Fig. 3). The prefix "V" denotes that all faces have identical edge valency.
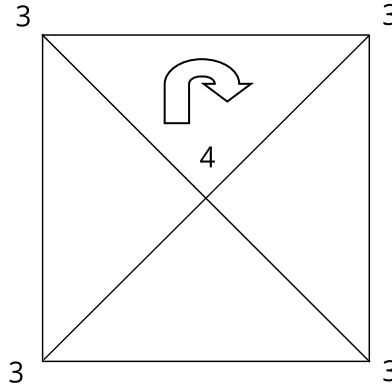
Figure 3: Nomenclature for a configuration by using the edge valency of the vertex. The edge valency is arranged in a clockwise direction to derive the nomenclature.

Three configurations (Fig. 4) with different edge valences were selected to study the effect of valency on the overall stability of reticulated domes. The nomenclature assigned for them based on the edge valency of the vertices is provided along with each configuration.

The faces near the support are different from the other regions of the dome configuration. Hence, the average value of edge valency of the vertices and edge valency of faces are introduced to capture the difference (Eq. 1 and Eq. 2). Those average values are calculated by considering the appropriate weight of each valency across the configuration. For Eq. 1, $\overline{V_1}$ is the average edge valency of the vertices, N_0^r is the number of vertices for which the edge valency is 'r' and N_0 is the number of vertices. For Eq. 2, $\overline{F_1}$ is the average edge valency of the faces, N_2^s is the number of faces for which the edge valency is 's', and N_2 is the number of faces in the configuration. The properties derived from parameters of dome configurations, including their average edge valency of the vertices and faces, are tabulated to identify the variation among them (Table 2).

$$\overline{V_1} = \sum_{r=2}^{n} \frac{rN_0^r}{N_0} \tag{1}$$

$$\overline{F_1} = \sum_{s=3}^{n} \frac{sN_2^s}{N_2} \tag{2}$$

5
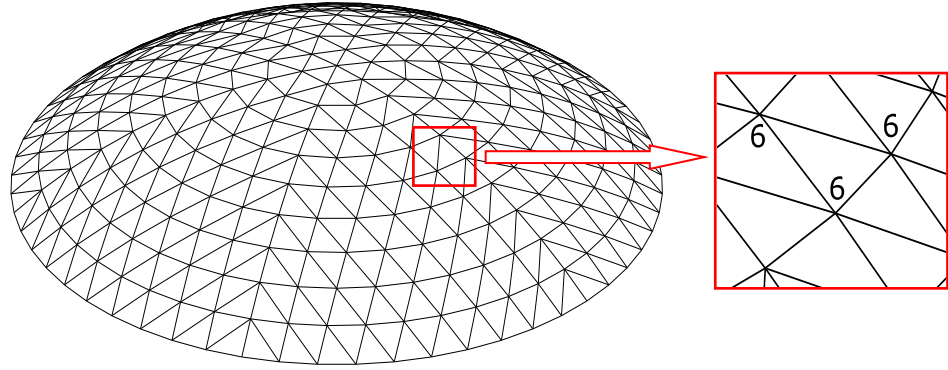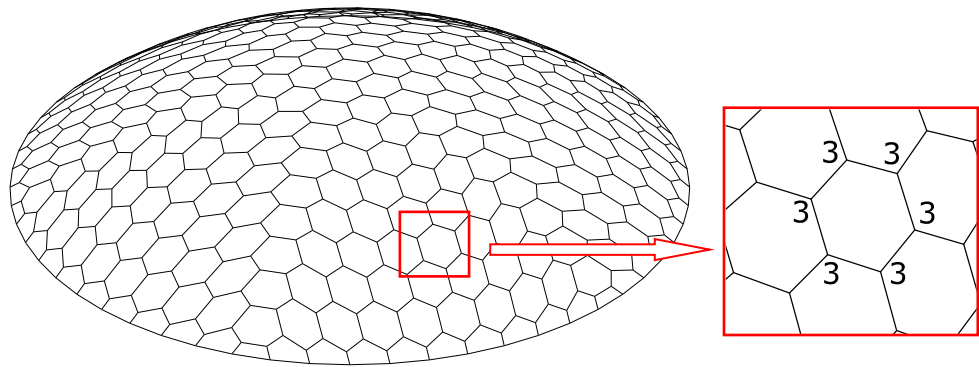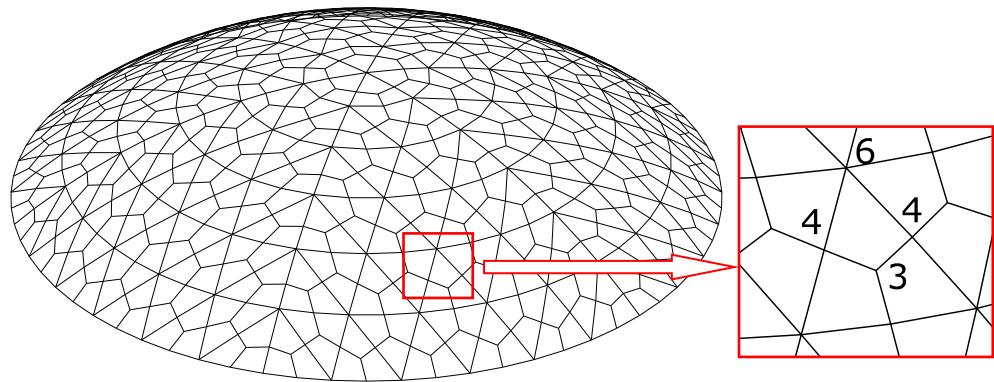
Figure 4: Three configurations with varied edge valency of the vertices and faces chosen for the study (a) V.6.6.6 (b) V.3.3.3.3.3.3 (c) V.6.4.3.4

Table 2: Properties of the three dome configurations

Parameters	V.6.6.6	V.3.3.3.3.3.3	V.6.4.3.4
N_0	331	660	685
N_1	930	990	1332
N_2	600	331	648
$\overline{V}_1$	5.620	3.0	3.889
$\overline{F}_1$	3.0	5.819	4.0

N_0 - Number of vertices, N_1 - Number of edges, N_2 - Number of faces,
$\overline{V}_1$ – Average edge valency of vertices, $\overline{F}_1$ - Average edge valency of faces

3. Limit load for the dome configurations

The three configurations were modeled and subjected to geometrical and material nonlinear analysis using the finite element software ABAQUS for finding the overall resistance. Domes with four rise-to-span ratios, two support conditions, and two loading patterns were used to establish the consistency of the results.

The span of the dome configurations is fixed at 40 meters, and the rise is varied to arrive at four different rise-to-span ratios (Fig. 5). They are denoted as R5, R6, R7, and R8 for the rise-to-span ratio of 1:5, 1:6, 1:7, and 1:8, respectively. Pin jointed and fixed support conditions are used for the dome configurations to find the effect of support conditions on the load capacity of the shells (Fig. 6). Two types of loading patterns were used to study the behavior of the dome. They are Full-span gravity loading and Semi-span gravity loading (Fig. 7). The unsymmetric loading is critical for the regions with high snowfall. Hence, semi-span gravity loading is considered during the analysis. The member cross-section is derived for the configurations based on IS 800 (2007) - Indian Code of practice for general construction in steel. The circular hollow section (CHS 125) of outer diameter 139.7 mm and thickness of 4.8 mm is adopted for all the members for the three configurations. The slenderness ratio of the members is adjusted to prevent the member buckling. The members are modeled with the Timoshenko beam element "B31" with four elements within a member. Elasto-perfectly plastic constitutive relation with the steel of young's modulus 200 GPa and yield stress 250 MPa is adopted for the model (Fig. 8). The members are assumed to have pure rigid connections between them. The pin-joint or semi-rigid joint is inadequate for the stability of single-layer dome configurations with non-triangulation as the primary cell. Hence, rigid connections are provided for all three dome configurations. The welding between the members helps to provide nearly rigid connections in real-world scenarios.

Based on the analysis of the three configurations under uniform gravity loading and the semi-span gravity loading, the limit load capacity of the configurations was obtained. The limit load is the apex of the load-deflection curve where the structure's stiffness will become zero. The member buckling is avoided in all the configurations by designing the members with an adequate slenderness ratio. As the weight of the structure is different among different configurations, the parameter 'λ' is defined by dividing the limit load by the total weight of the structure (Eq. 3). Here, 'P' is the limit load (kN), and 'w' is the total weight (kN) of the structure.

$$\lambda = \frac{P}{w}$$

(3)
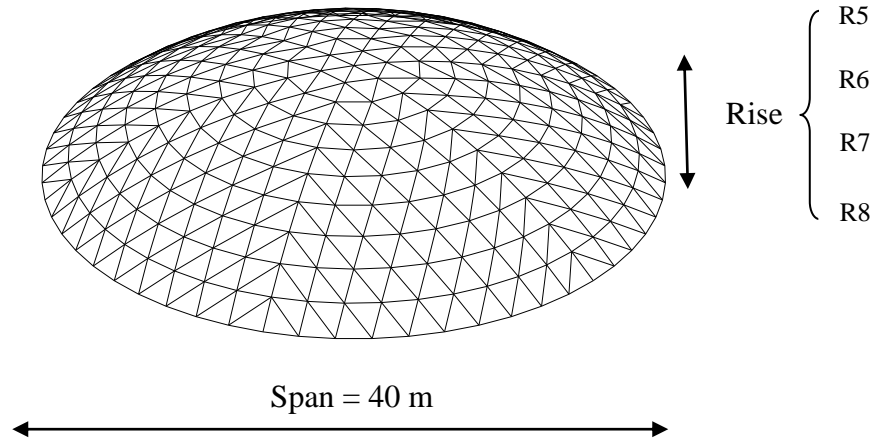
Figure 5: The dome configuration with a span of 40 meters. The span-to-rise ratios varied from 5 to 8.

(a)   (b)
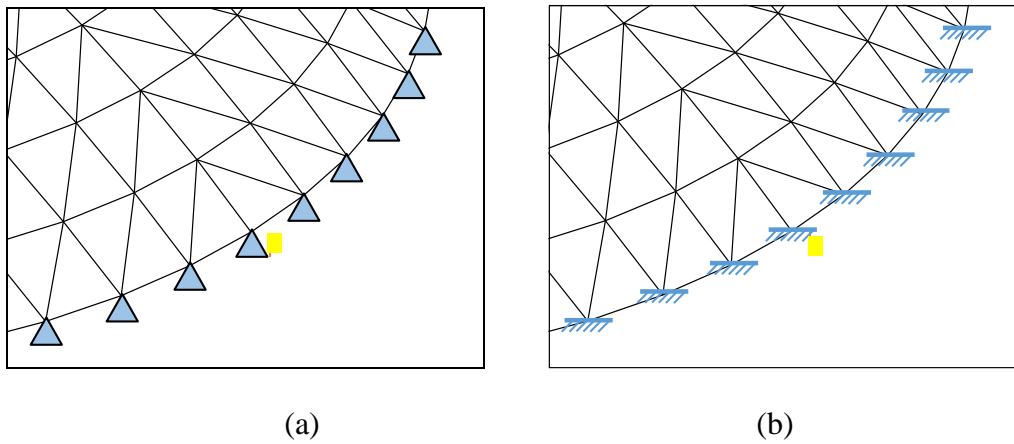
Figure 6: Support conditions adopted for the study: (a) Pin jointed support (b) Fixed support

(a)   (b)
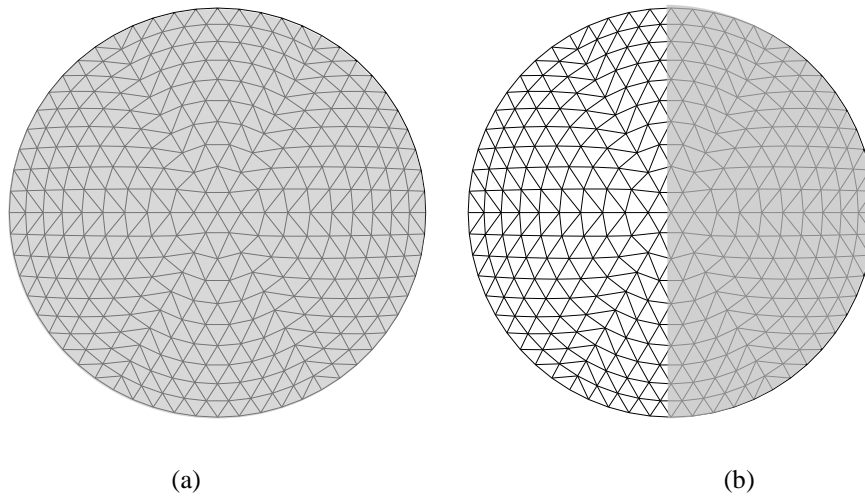
Figure 7: Loading patterns considered for the study: (a) Full-span gravity loading (b) Semi-span gravity loading
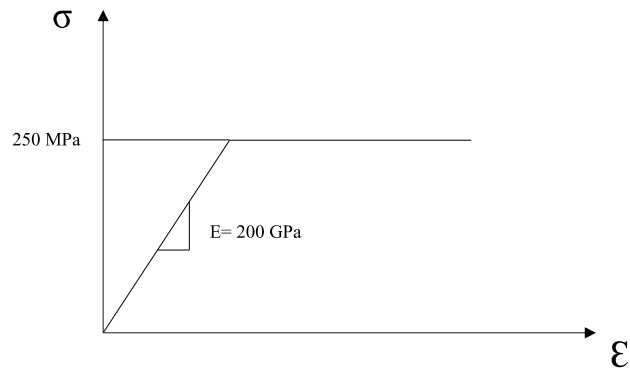
Figure 8: Elasto- perfectly plastic constitutive model for studying the behavior under gravity loading
(σ - Stress in MPa, ε - Strain, and E - Young's modulus in MPa)

The three given dome configurations have a different value of average edge valency of vertices and average edge valency of faces. The impact of support conditions on the limit load capacity is different among the three dome configurations. The variation in limit load capacity with support conditions is minimum for configuration V.6.6.6 and maximum for configuration V.3.3.3.3.3.3 when full-span gravity loading is considered (Fig. 9). However, this variation is minimal for all three configurations when semi-span gravity loading is considered (Fig. 10). Hence, the impact of support conditions is higher for the dome configuration with full-span gravity loading compared to semi-span gravity loading. This impact is minimal for configuration V.6.6.6, where the average edge valency of the vertices is high, and the average edge valency of the face is low. The minimum impact of support conditions is explained by the triangulation present in this configuration, which avoids the requirement of rigid fixity of bases in real structures.
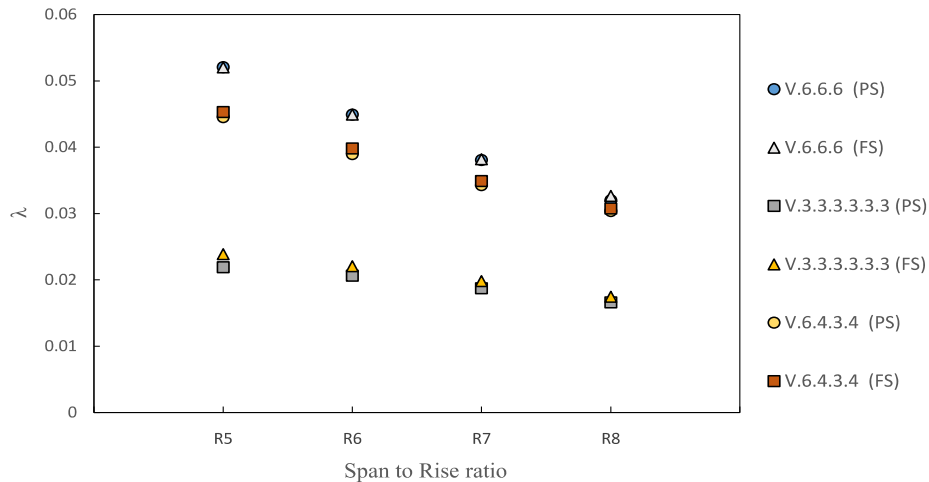
Figure 9: Comparison of limit load capacity using λ for different support conditions with full-span gravity loading
(PS: Pinned support, FS: Fixed support)

9
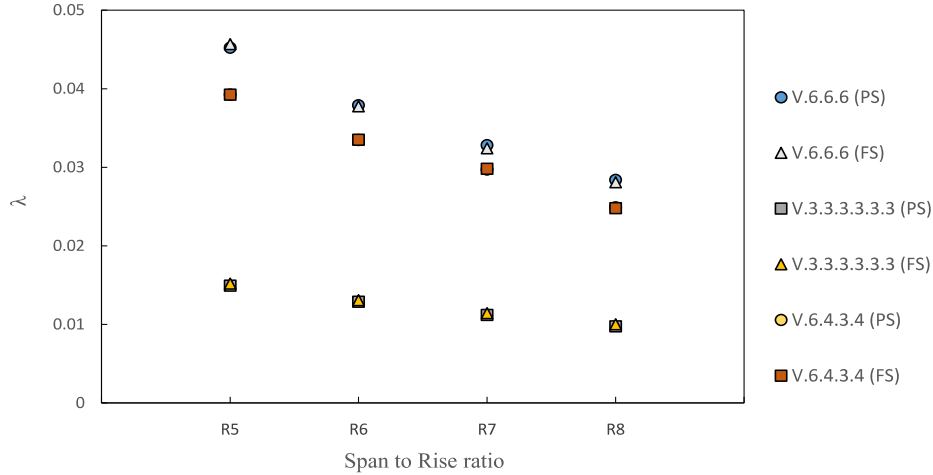
Figure 10: Comparison of limit load capacity using λ for different support conditions with semi-span gravity loading (PS: Pinned support, FS: Fixed support)

The impact of loading patterns on dome configurations was studied by considering full-span gravity loading and semi-span gravity loading. The study of unsymmetrical loading is critical for regions with heavy snowfall, where the unsymmetrical distribution of snow load can cause the failure of dome structures. The variation in the parameter λ was studied by considering various rise-to-span ratios and the two support conditions. The reduction in load capacity is minimum for configuration V.6.6.6 and maximum for configuration V.3.3.3.3.3.3 when the dome was subjected to semi-span gravity loading compared to full-span gravity loading with pin support (Fig. 11). This reduction was less for dome configurations with rigid supports than for dome configurations with pin supports due to the higher rigidity provided by the fixed supports (Fig. 12). Overall, the load capacity is higher for configuration V.6.6.6 and lower for configuration V.3.3.3.3.3.3. This observation reinstates the impact of higher average edge valency of vertices and lower edge valency of faces on the overall stability of the dome configuration.
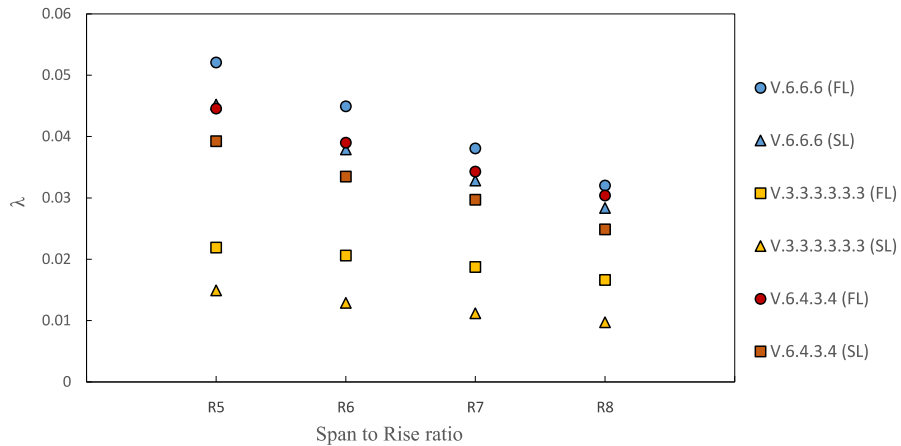
Figure 11: Comparison of limit load capacity using λ for different loading conditions with pinned support (FL: Full span gravity loading, SL: Semi span gravity loading)

10
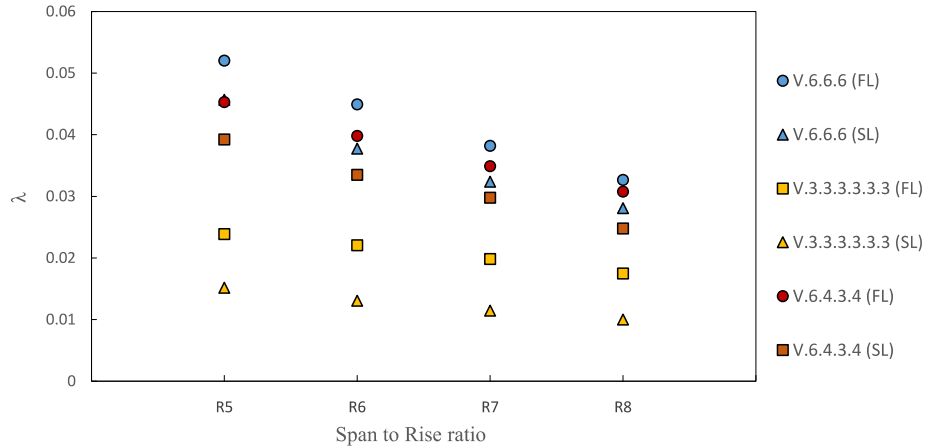
Figure 12: Comparison of limit load capacity using λ for different loading conditions with fixed support
(FL: Full span gravity loading, SL: Semi span gravity loading)

The impact of the average edge valency of the vertices and the average edge valency of the faces on the limit load of the dome configurations was studied by considering the limit load parameter λ. Results were linked for dome configurations with two support conditions, four rise-to-span ratios, and two loading cases. The arrived outcomes were fitted with a second-degree polynomial to comprehend the trend of λ with the average edge valency.

The limit load capacity increases with the increase in the average edge valency of the vertices for dome configurations with both pin support conditions and fixed support conditions under full-span gravity loading (Fig. 13(a) & Fig. 13(c)). The maximum limit load capacity is for the configuration with average edge valency of the vertices 5.62, and the least limit load capacity is for 3. However, the limit load capacity decreases with an increase in the average edge valency of the faces (Fig. 13(b) & Fig. 13(d)).

The support change has minimal impact on the limit load capacity for the configuration with nomenclature V.6.6.6 and maximum impact for the configuration with nomenclature V.3.3.3.3.3.3. This difference shows the superiority of triangulation even though the member connections are rigid.

The results obtained for dome configurations under semi-span gravity loading were similar to the full-span gravity loading case. The λ increases with the average edge valency of the vertices and decreases with the average edge valency of the faces (Fig. 14). The difference was only the reduction in the limit load capacity (hence the value of λ) for semi-span loading compared to the full-span loading case.

Hence, the analysis shows a trend among the selected single-layer dome configurations. Increasing the average edge valency of the vertices and decreasing the average edge valency of the vertices increases the stability of the single-layer dome configurations.
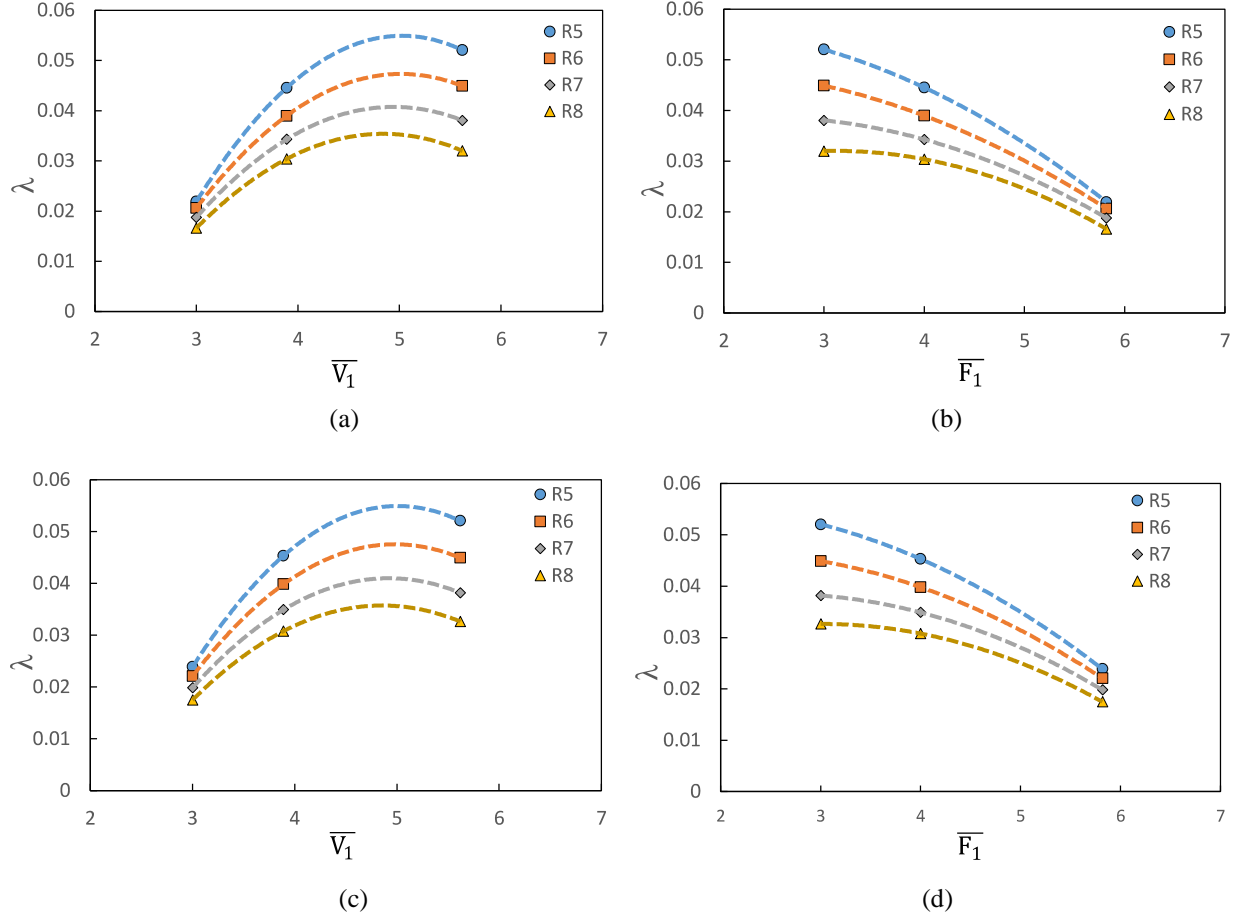
Figure 13: The variation of limit load capacity of the dome configurations in terms of the parameter λ with the average edge valency of the vertices and the average edge valency of the faces under full-span gravity loading: (a) comparison with average edge valency of vertices for the domes with pinned support condition (b) comparison with average edge valency of faces for the domes with pinned support condition (c) comparison with average edge valency of vertices for the domes with fixed support condition (d) comparison with average edge valency of faces for the domes with fixed support condition

4. Discussion

The effect of edge valency of the vertices and edge valency of faces on the structural stability of the given single-layer shell configurations was proposed by comparing the limit load with the average edge valency. The results were obtained for dome configurations with the different rise-to-span ratios, the support conditions, and the loading cases. As the weight of the structures was not identical among the three configurations, a parameter λ was used to compare the dome configurations' stability.

The limit load capacity increases with the increase in the average edge valency of the vertices and decreases with the increase in the average edge valency of the faces. This result was found to be valid irrespective of the two support conditions, the rise of the structure and the loading pattern. The higher value of the average edge valency provides more rigidity to the joint system and increases the stability of the configuration. On the other hand, the increase in the average edge valency of the faces reduces the planar rigidity of the faces, which reduces the buckling load of the structure. Both the valences (edge valency of vertices and edge valency of faces) are

mutually dependent. When the edge valency of vertices increases for a configuration, the edge valency of faces reduces automatically to satisfy the configuration uniformity. Hence, the higher edge valency of vertices, which results in the lower edge valency of faces, increases the stability of the dome configuration.

The impact of edge valency is very high for structures like single-layer domes, where the number of members used is very high compared to any other structure. Deciding the optimum valency will reduce the number of members and the fabrication, which will reduce the overall cost of the system. Optimizing the valency also increases the lightness of the structure and saves the construction materials. The optimized configuration can have sufficient redundancy so as not to compromise stability. It requires rigorous study of the configurations with several iterations to optimize resistance and material utilization.

(a)

(b)

(c)

(d)
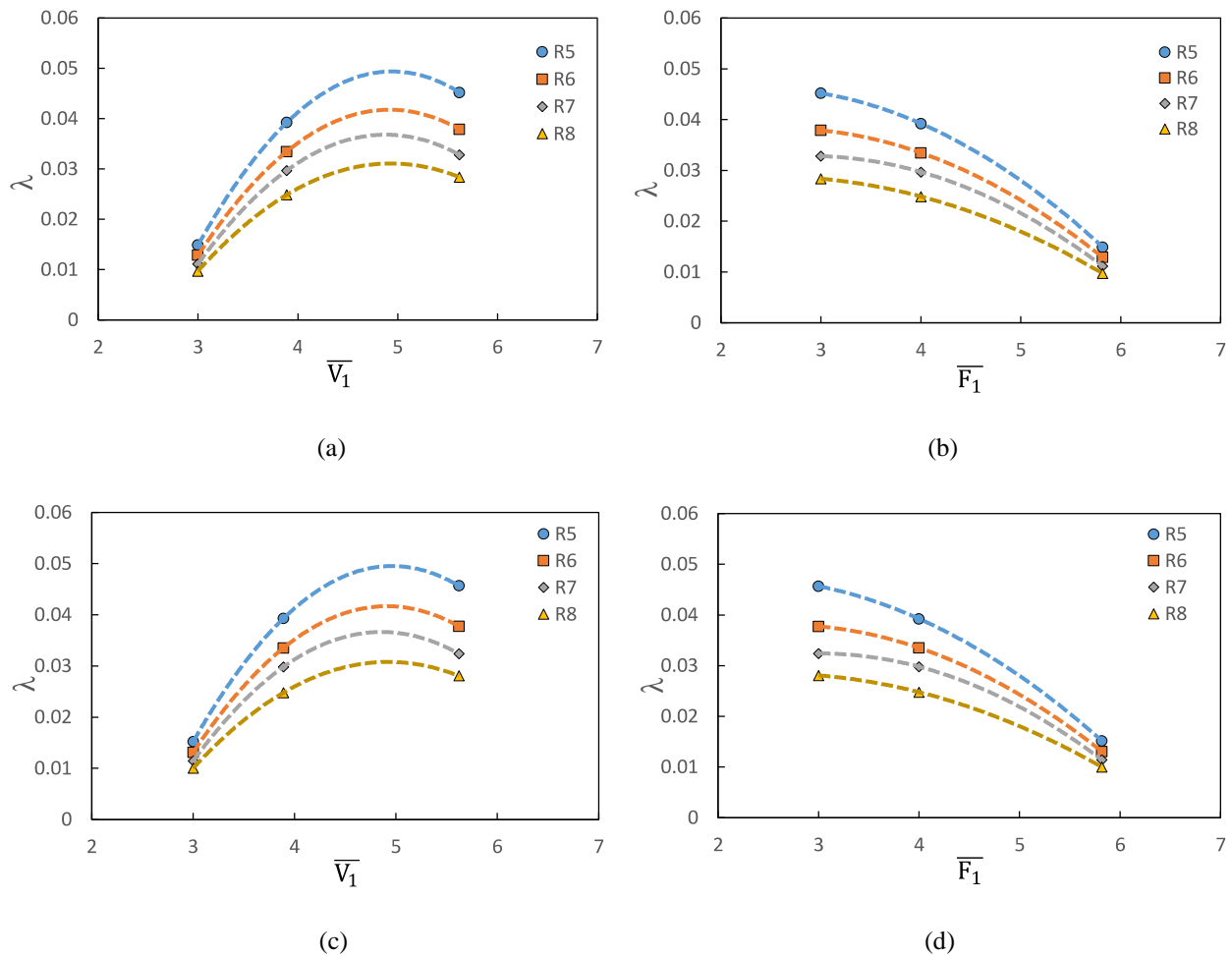
Figure 14: The variation of limit load capacity of the dome configurations in terms of the parameter λ with the average edge valency of the vertices and the average edge valency of the faces under semi-span gravity loading: (a) comparison with average edge valency of vertices for the domes with pinned support condition (b) comparison with average edge valency of faces for the domes with pinned support condition (c) comparison with average edge valency of vertices for the domes with fixed support condition (d) comparison with average edge valency of faces for the domes with fixed support condition

The present study considers the edge valency of vertices and the edge valency of faces. Even though the parameter λ helps to nullify the difference in the weight of the structure, the number of members and the joints used are different for the three configurations (Table 2). These additional parameters also play a crucial role in the stability of the domes. The variation in member lengths across configurations is kept as minimum as possible. However, individual member lengths are different across the three configurations. As the critical load is governed by its effective length, variation in the individual member length also contributes to the stability of dome configurations, which was not considered in this study. The members are rigidly connected for the three single-layer configurations. As the number of vertices is different, the global stability of the dome configurations is affected by the number of vertices. A multi-level optimization helps to include these parameters together. However, it is difficult to understand which parameter affects what as optimizing one will vary the others. For example, keeping the number of edges equal in the three configurations will result in massive differences in vertices and faces. Hence, considering the effect of all the parameters in a single study is complex and avoided in the present study.

The advantages of bringing the parameters (vertices, edges, and faces) into the stability of the dome configurations are many. Optimizing the chosen parameters will help to reduce the redundancy of the structure without compromising stability and overall load resistance. For example, the complete triangulated system with rigid joints is not required when the load requirement of the domes is not high. The study of edge valency will optimize the faces, which helps to reduce the number of connections and members. The rigorous analysis of the parameters can reduce the dependency on commercial software packages to study reticulated domes' performance. Different design parameters such as load capacity can be qualitatively and quantitatively examined with defined parameters as the variable inputs. Hence, further studies on parameters such as valency and dimensionality are helpful in the optimum design of reticulated structures such as domes.

5. Concluding remarks
The effect of edge valency on the overall resistance of single-layer reticulated steel domes is studied by considering three configurations with varying parameters. The effect of support conditions, unsymmetrical loading on the structure, and the change in rise-to-span ratios are analyzed while studying the dependence of limit load on the edge valency of vertices and edge valency of faces. The significant conclusions arrived from this study are:

- The overall resistance of the dome configuration increases when the edge valency of the vertices increases and the edge valency of the faces decreases. The increase in edge valency of the vertices increases joint stiffness, and reducing face valency increases the in-plane stiffness of the structure. As dome structures are doubly curved, both factors influence the structure's overall stability.
- The impact of support rigidity is least for configuration V.6.6.6 and high for configuration V.3.3.3.3.3.3. Hence, vertices with high average edge valency provide maximum stability and reduce dependence on support rigidity.
- Unsymmetrical loading reduces the overall resistance of the structure compared to full span gravity loading. The reduction in the load capacity with unsymmetrical loading is

minimal for configurations with high average edge valency of the vertices and low average edge valency of the faces.

References

Abaqus CAE (2009). *Standard User's Manual*, Version 6.9, Dassault Systemes Simulia.

Abedi, K., & Parke, G. A. R. (1996). Progressive collapse of single-layer braced domes. *International Journal of Space Structures*, *11*(3), 291-306.

Fan, F., Cao, Z., & Shen, S. (2010). Elasto-plastic stability of single-layer reticulated shells. *Thin-Walled Structures*, *48*(10-11), 827-836.

Fan, F., Yan, J., & Cao, Z. (2012). Elasto-plastic stability of single-layer reticulated domes with initial curvature of members. *Thin-Walled Structures*, *60*, 239-246.

Geometrica Inc (2008, August 6). *Cemex Merida 86m limestone dome* [Photograph]. Flickr. Retrieved from https://www.flickr.com/photos/geometricainc/6956742455/in/album-72157629155703184

Gioncu, V., & Balut, N. (1992). Instability behaviour of single-layer reticulated shells. *International journal of space structures*, *7*(4), 243-252.

IASS, WG 8. (2014). Guide to Buckling Load Evaluation of Metal Reticulated Roof Structures (Report of Activities WG 8). *International Association for Shell and Spatial Structures*.

IS 800 (2007). General construction in steel-code of practice. *3rd Revision, Bureau of Indian Standard,* New Delhi, India.

Kani, I. M., & Heidari, A. (2007). Automatic two-stage calculation of bifurcation path of perfect shallow reticulated domes. *Journal of Structural Engineering*, *133*(2), 185-194.

Kato, S., Mutoh, I., & Shomura, M. (1998). Collapse of semi-rigidly jointed reticulated domes with initial geometric imperfections. *Journal of constructional steel research*, *48*(2-3), 145-168.

Kolakkattil, R., & Jayachandran, A. (2021). Global Stability Behavior of Single-Layer Reticulated Domes Created Using a New Nomenclature. *Journal of the International Association for Shell and Spatial Structures*.

Kolakkattil, R., Tsavdaridis, K. D., & Sanjeevi, A. J. (2021). Influence of edge valencies on the overall resistance of single-layer reticulated cylindrical shells. In *Proceedings of the IASS Annual Symposium 2020/21*. IASS.

Lenza, P. (1992). Instability of single layer doubly curved vaults. *International Journal of Space Structures*, *7*(4), 253-264.

Loeb, A. (2012). *Space structures: Their harmony and counterpoint.* Springer Science & Business Media.

López, A., Puente, I., & Serna, M. A. (2007). Direct evaluation of the buckling loads of semi-rigidly jointed single-layer latticed domes under symmetric loading. *Engineering structures*, *29*(1), 101-109.

López, A., Puente, I., & Serna, M. A. (2007). Numerical model and experimental tests on single-layer latticed domes with semi-rigid joints. *Computers & structures*, *85*(7-8), 360-374.

Ma, H., Fan, F., Wen, P., Zhang, H., & Shen, S. (2015). Experimental and numerical studies on a single-layer cylindrical reticulated shell with semi-rigid joints. *Thin-Walled Structures*, *86*, 1-9.

Makowski, Z. S. (Ed.). (1986). *Analysis, design, and construction of braced barrel vaults*. CRC Press.

Nooshin, H., & Disney, P. (2000). Formex configuration processing I. *International journal of space structures*, *15*(1), 1-52.

Saitoh, M., Hangai, Y., Toda, I., Yamagiwa, T., & Okuhara, T. (1986, September). Buckling loads of reticulated single-layer domes. In *Proceedings of IASS Symposium* (Vol. 3, pp. 121-128).

Suzuki, T., Ogawa, T., & Ikarashi, K. (1992). Elastic buckling analysis of rigidly jointed single-layer reticulated domes with random initial imperfection. *International Journal of Space Structures*, *7*(4), 265-273.

Tanaka, K., Kondoh, K., & Atluri, S. N. (1985). Instability analysis of space trusses using exact tangent-stiffness matrices. *Finite elements in analysis and design*, *1*(4), 291-311.

Tsavdaridis, K. D., Feng, R., & Liu, F. (2020). Shape Optimization of Assembled Single-Layer Grid Structure with Semi-Rigid Joints. *Procedia Manufacturing*, *44*, 12-19.

Tsuboi, Y. (1984). Analysis, design, and realization of space frames: a state-of-the-art report. *Bull. International Association for Shell and Spatial Structures*, (84/85)

Yamada, S., Takeuchi, A., Tada, Y., & Tsutsumi, K. (2001). Imperfection-sensitive overall buckling of single-layer lattice domes. *Journal of Engineering Mechanics*, *127*(4), 382-386.

Yan, J., Qin, F., Cao, Z., Fan, F., & Mo, Y. L. (2016). Mechanism of coupled instability of single-layer reticulated domes. *Engineering Structures*, *114*, 158-170.